REMARKS

The claims remaining in the application are 1-17.

Rejection Under 35 U.S.C. § 102

The Office Action has rejected claims 1-4, 7-12, and 14-16 under 35 U.S.C. 102(e) as being anticipated by U.S. Patent 6,512,994 (Sachdeva). This rejection is respectfully traversed.

Rejection Under 35 U.S.C. § 103

The Office Action has rejected claims 5, 6, and 13 under 35 U.S.C. 103(a) as being unpatentable over U.S. Patent 6,512,994 (Sachdeva) in view of U.S. Patent 6,648,640 (Rubbert et al.). This rejection is respectfully traversed.

The Office Action has rejected claim 17 under 35 U.S.C. 103(a) as being unpatentable over U.S. Patent 6,512,994 (Sachdeva). This rejection is respectfully traversed.

Comments

The claims have been amended to further narrow the scope of the claims and more truly distinguish the patentable invention from the references cited. No new matter has been added.

As spelled out in the revised claims the present invention differs significantly from Sachdeva. Some specific differences are the use of the 3-dimensional intra-oral target, this is shown in Figure 2 of the present invention. The 3-dimensional intra-oral target allows the use of photogrammetry to capture a precise series of images, from non-orthogonal positions, to construct an accurate model. It is clear, as discussed in more detail in the paragraph below, that photogrammetry is clearly different from the single scaling factor used in Sachdeva.

The physical model of the sensor used in the present invention is superior to the method in Sachdeva, specifically in the ability to correct for sources of error beyond scale. The analytical representation of the physical model, includes multiple parameters that model the imaging process. These include parameters for camera position, orientation, interior construction (e.g., focal length), and lens distortion parameters. In addition to correcting for sources

of error beyond scale, the parameters allow corrections to be applied differentially across an image. This is clearly different from the single scale factor used by Sachdeva and of particular importance in this application where scale and other errors vary significantly across the imaged scene. This variation is due to the close-range nature of the image capturing event, i.e. the camera is focused at a finite distance, and the use of non-metric cameras. The formulation of the physical model is well known to those of ordinary skill in this art and described, e.g., in the Manual of Photogrammetry, Fourth Edition, op. cit., pp. 48-54 and pp. 244-247. Methods for correcting lens distortion in a close range situation are described pp. 258-260.

CONCLUSION

Dependent claims not specifically addressed add additional limitations to the independent claims, which have been distinguished from the prior art and are therefore also patentable.

In conclusion, none of the prior art cited by the Office Action discloses the limitations of the claims of the present invention, either individually or in combination. Therefore, it is believed that the claims are allowable.

If the Examiner is of the opinion that additional modifications to the claims are necessary to place the application in condition for allowance, he is invited to contact Applicant's attorney at the number listed below for a telephone interview and Examiner's amendment.

Respectfully submitted,

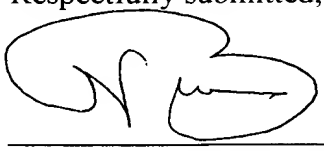

Attorney for Applicant(s)
Registration No. 29,134

Nelson A. Blish/tmp
Rochester, NY 14650
Telephone: 585-588-2720
Facsimile: 585-477-4646

If the Examiner is unable to reach the Applicant(s) Attorney at the telephone number provided, the Examiner is requested to communicate with Eastman Kodak Company Patent Operations at (585) 477-4656.

Manual of Photogrammetry

Fourth Edition

Editor-in-Chief
Chester C Slama

Associate Editors
Charles Theurer
Soren W. Henriksen

American Society of Photogrammetry

Fourth Edition

Library of Congress Cataloging in Publication Data

American Society of Photogrammetry.
Manual of Photogrammetry.

Includes index.
1. Photographic surveying—Handbooks, manuals, etc.
2. Photogrammetry—Handbooks, manuals, etc. I. Slama, Chester C
II. Theurer, Charles. III. Henriksen, Soren W. IV. Title.
TA593.25.A48 1980 526.9'82 80-21514
ISBN 0-937294-01-2

PUBLISHED BY
AMERICAN SOCIETY OF PHOTOGRAMMETRY
105 N. Virginia Ave.
Falls Church, Va. 22046

measured on the photograph. Whether stereoscopic parallax or a plotting instrument is implied, relief displacement is the fundamental element that makes height determination possible. The desired elevation differences, together with the corresponding displacements, are relatively small quantities. For example, the relief displacement for a 10-metre contour interval where the flight height is 6,000 metres and where the image is 30 mm from the center, is only 0.05 mm. The small size of the quantity causes it to be difficult to measure accurately. If, in addition, the value of the apparent displacement of an image is combined with a totally unrelated tilt displacement that can be larger than the relief displacement, an accurate analysis of the effect is very complicated. The simplest instrument made to assist in solving the problem in a comparatively crude, near-accurate manner costs a few hundred dollars, whereas an instrument that gives a complete and accurate solution costs a few tens of thousands of dollars. Graphic methods are not applicable, but analytic computations are coming into common use.

2.2.2.6 Tilt Determination

The tilt of an aerial photograph can be computed if the ground position of three or more image points in the photograph are known. The Church Method of space resection, which will be described in section 2.2.4.2, is suitable for tilt determination using either desk or electronic computers. This method has sufficient accuracy for most practical applications relating to photo-interpretation and quantitative analysis. If a large number of control points are available, then the method of least squares adjustment may be applied. The mathematical solution for the simultaneous solution of large photogrammetric blocks, which will be presented in section 2.6, may also be used to determine the tilts of all the photographs which provide complete stereoscopic coverage of an area.

Several other methods of tilt determination were discussed in chapter II of the Third Edition of the Manual of Photogrammetry. These methods included: (1) the image-displacement method; (2) the Anderson scale-point method; and (3) the Morse Method. These methods are not in common use and interested readers are referred to the previous edition of this Manual.

2.2.3 CONCEPTS OF ORIENTATION

The geometric principle of stereophotogrammetry is illustrated in figure 2-8. The area to be mapped is photographed from two different camera positions, O_L and O_R. The area of common coverage by the two photographs is called stereoscopic overlap. Each photograph may be considered as a record of the bundle of light rays which travel from the object space, pass through the nodal point of the camera lens system, and register on the photographic film. In the laboratory, an optical model of the stereoscopic overlap area can be constructed in an instrument called stereoplotter. Each bundle of rays is reconstructed by inserting either a glass plate diapositive or film negative into a projector. The process of reconstructing the internal geometry of the bundle of rays in a projector is called interior orientation. The two projectors may each be translated and tilted until they assume the same relative position and attitude as that of the camera in its two positions during the photography. This process is called relative orientation. At the completion of relative orientation, corresponding light rays in the two bundles intersect in space and a three-dimensional optical model is formed. Finally, in a process called absolute orientation, points of known ground positions (called control points) are used to scale the model and to level it with respect to the reference plane in the instrument. Once absolute orientation is completed, the position of any point in the stereo model may be measured at the intersection of the two corresponding rays from the two projectors. Further details on the operation and principle of the stereoplotters will be included in chapters XI and XII.

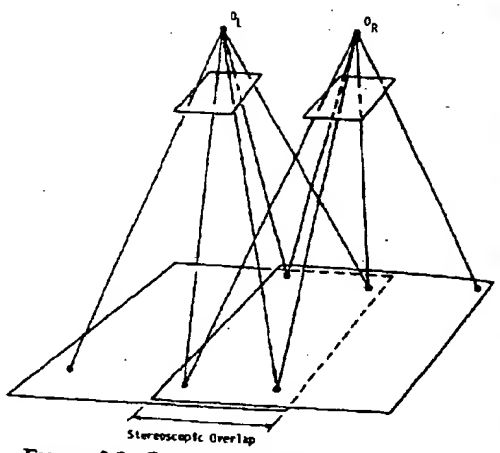

Figure 2-8. Geometry of stereoscopic coverage.

In computational photogrammetry, the path of each ray of light may be described by a mathematical expression which is a function of the position of the point in the object space, position of the image point in the photograph, position of the exposure center in the ground reference system, direction of the optical axis of the camera and the perspective geometry of the camera. If the perspective geometry of the camera has been determined by camera calibration and if three or more control points are imaged on a photograph, the position of the camera and its attitude with respect to the ground control reference system can be deter-

mined. Once the orientation of both of the photographs of a stereoscopic pair is known, the position of any object point which is located in the overlap area may be computed as the point of intersection of two rays.

Therefore, in both the instrumental and analytical approach of photogrammetric measurements, determination of the orientation of the camera at the moment of exposure is a necessary step in the measurement process. There are basically four orientation problems: (1) interior orientation; (2) exterior orientation; (3) relative orientation; and (4) absolute orientation.

2.2.3.1 Interior Orientation

The interior orientation of a camera refers to the perspective geometry of the camera and is defined by the following parameters: (1) the calibrated focal length; (2) the position of the principal point in the image plane; and (3) the geometric distortion characteristics of the lens system. The interior orientation of a camera can be determined by either field or laboratory calibration procedure (*see* chapter IV).

2.2.3.1.1 Purpose of Fiducial Marks

An aerial mapping camera is equipped with either four or eight fiducial marks which are permanently mounted in the camea housing and located in front of the image plane. Images of the fiducial marks appear on each photograph. The primary purpose of the fiducial marks is to define the location of the principal point of the photograph. The fiducial marks are positioned so that the intersection of the lines joining diametrically opposite fiducial marks coincide with the principal point. In stereoplotting instruments, the plate carriage in each projector are also equipped with at least four fiducial marks which define the position of the principal point in the carriage plate. Thus, by positioning the photographic plate on the carriage so that the fiducial marks on the photographic plate coincides with those in the carriage, the photograph is centered properly with respect to the optical axis of the projector.

2.2.3.1.2 Photo-Coordinate System

Figure 2-9 illustrates a three-dimensional photo-coordinate system ($\bar{x}$, $\bar{y}$, $\bar{z}$) which is commonly used to define the location of image points with respect to the exposure center, O. In the plane of the photograph, point O' is the point of intersection of the lines joining fiducial marks A and C and B and D. If the four fiducial marks are perfectly aligned, the lines AC and BD should be orthogonal with each other and the point of intersection (O') should be in coincidence with the principal point. This condition is difficult to achieve in practice. For the purpose of generality, the x-axis on the plane of the photograph is defined as the line joining

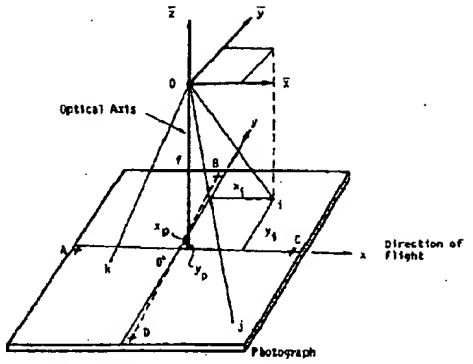

Figure 2-9. A photo-coordinate system.

point O' and fiducial mark C. The positive x-axis points in the general direction of flight of the aircraft. The y-axis passes through O' and is perpendicular to the x-axis.

The photo-coordinate system is defined by the axes $\bar{x}$, $\bar{y}$ and $\bar{z}$ with the origin of the system situated at the exposure center (O). The $\bar{z}$-axis coincides with the optical axis of the camera and is positive along the direction towards the image plane of the camera. The $\bar{x}$-axis is parallel to the x-axis on the plane of the photograph and is positive towards the direction of flight. The $\bar{y}$-axis is parallel to the y-axis on the photographic plane. Thus, the $\bar{x}$-$\bar{y}$ plane is parallel to the photographic plane. Assuming that the principal point is not exactly in coincidence with point O', its position on the plane of the photograph is then defined by its coordinates x_p and y_p. The position of an image point i in the same plane can be defined by its coordinates x_i and y_i. The position of the same image point with respect to the exposure center (O) is then defined by its photo-coordinates $\bar{x}_i$, $\bar{y}_i$ and $\bar{z}_i$ as follows:

$$\begin{aligned} \bar{x}_i &= x_i - x_p \\ \bar{y}_i &= y_i - y_p \\ \bar{z}_i &= -f \end{aligned} \tag{2.19}$$

2.2.3.1.3 Mathematical Definition of Interior Orientation

The interior orientation of a photogrammetric camera is said to be mathematically defined if the following parameters are known:

(1) focal length, f;
(2) coordinates of the principal point, x_p and y_p; and
(3) geometric distortion characteristics of the lens system.

One commonly used model for correcting lens distortion is that developed by D. Brown:

$$\begin{aligned} \Delta x_i = {} & \bar{x}_i[l_1 r^2 + l_2 r^4 + l_3 r^6] \\ & + [p_1(r^2 + 2\bar{x}_i^2) + 2p_2 \bar{x}_i \bar{y}_i][1 + p_3 r^2] \end{aligned} \tag{2.20}$$

$$\Delta y_j = \bar{y}_j\left[l_1 r^2 + l_2 r^4 + l_3 r^6\right] + \left[2p_1\bar{x}_j\bar{y}_j + p_2\left(r^2 + 2\bar{y}_j^2\right)\right]\left[1 + p_3 r^2\right]$$

where Δx_j and Δy_j are corrections for geometric lens distortions present in the coordinates $\bar{x}_j$ and $\bar{y}_j$ of image point j; and $r = (\bar{x}_j^2 + \bar{y}_j^2)^{1/2}$. The coefficients l_1, l_2, l_3, p_1, p_2 and p_3 may be determined as a part of the camera calibration process. The model accounts for both symmetric radial distortion and asymmetric distortions caused by lens decentering. The terms which include the coefficients l_1, l_2 and l_3 represent symmetric radial distortion, and the terms which include p_1, p_2 and p_3 represent asymmetric distortion.

The photo-coordinates are corrected for lens distortion by the following expression:

$$\bar{x}_j' = \bar{x}_j + \Delta x_j$$
$$\bar{y}_j' = \bar{y}_j + \Delta y_j. \qquad (2.21)$$

2.2.3.2 Exterior Orientation

The exterior orientation of a camera during the moment of exposure of a particular photograph is defined by the geographic position of the exposure center and the direction of the optical axis. In computational photogrammetry, the geographic position of the exposure center is most conveniently defined by its coordinates in a three-dimensional rectangular coordinate system, and the direction of the optical axis is usually defined by three rotation angles (either ω, ϕ and κ or tilt, swing and azimuth).

2.2.3.2.1 A Three-Dimensional Rectangular Coordinate System

Figure 2-10 shows that the locations of points in the object space may be defined by a three-dimensional rectangular coordinate system. The origin and orientation of the coordinate system may be arbitrarily defined. In analytical aerotriangulation, the origin is usually chosen to be located near the center of the area of concern so that the number of digits in each coordinate number can be kept at a minimum. The positive Y-axis is usually directed towards true north. The location of any point j in the object space can therefore be defined by its three coordinates X_j, Y_j and Z_j. The position of the exposure center of a photograph can similarly be defined by its coordinates X_i^c, Y_i^c and Z_i^c.

In geodetic surveying, the positions of survey stations are usually defined in geographic coordinates (longitude, latitude, and elevation above mean sea level), or in a state plane coordinate system (X, Y, and elevation above mean sea level). Neither of these coordinate systems are convenient for computation purposes. When geodetic control points are defined in either one of these coordinate systems, their coordinates are usually first transformed to a locally defined rectangular coordinate system.

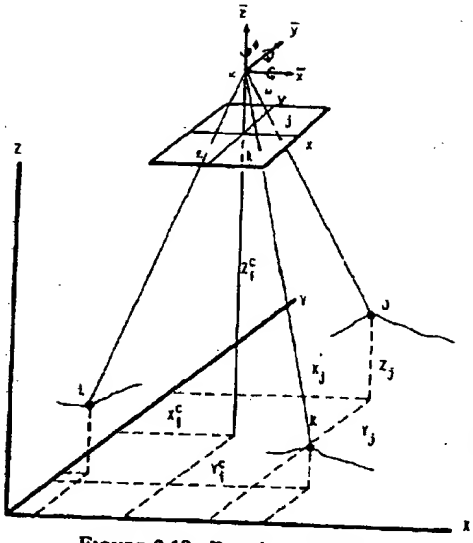

Figure 2-10. Exterior orientation.

The definition of various ground reference coordinate systems and transformation equations for converting from one system to the other are given in chapter VII.

2.2.3.2.2 Omega (ω), Phi (ϕ) and Kappa (κ)

As the spatial position of the exposure center is defined by its coordinates X_i^c, Y_i^c and Z_i^c, the direction of the optical axis may be defined by the rotation angles omega (ω), phi (ϕ) and kappa (κ) about the $\bar{x}$-, $\bar{y}$- and $\bar{z}$-axis respectively of the photo-coordinate system. All the rotations are defined positive in the counterclockwise direction. When $\omega = \phi = \kappa = 0$, the optical axis is perpendicular to the X-Y plane and the $\bar{x}$-, $\bar{y}$- and $\bar{z}$- axis are parallel to the X-, Y- and Z-axis respectively. However, it should be noted that because of the curvature of the earth's surface, zero rotation about the $\bar{x}$-, $\bar{y}$- and $\bar{z}$-axis does not mean that the photograph is truly vertical.

2.2.3.2.3 Projective Transformation Equations

Assuming that light rays travel in straight lines, that all the rays entering a camera lens system pass through a single point and that the lens system is distortionless, then a projective relationship exists between the photographic coordinates of the image points and the ground coordinates of the corresponding object points as illustrated in figure 2-10. It will be shown in this section that this projective relationship can be represented by the following set of projective transformation equations:

$$X_j - X_i^c = \lambda_{ij}\left[m_{11}(x_{ij} - x_p) + m_{21}(y_{ij} - y_p) + m_{31}(-f)\right]$$

$$Y_j - Y_i^c = \lambda_{ij}\,[m_{12}\,(x_{ij} - x_p) + m_{22}\,(y_{ij} - y_p) + m_{32}\,(-f)] \quad (2.22)$$

$$Z_j - Z_i^c = \lambda_{ij}\,[m_{13}\,(x_{ij} - x_p) + m_{23}\,(y_{ij} - y_p) + m_{33}\,(-f)]$$

in which

$$\begin{aligned}
m_{11} &= \cos\phi_i \cos\kappa_i \\
m_{12} &= \cos\omega_i \sin\kappa_i + \sin\omega_i \sin\phi_i \cos\kappa_i \\
m_{13} &= \sin\omega_i \sin\kappa_i - \cos\omega_i \sin\phi_i \cos\kappa_i \\
m_{21} &= -\cos\phi_i \sin\kappa_i \\
m_{22} &= \cos\omega_i \cos\kappa_i - \sin\omega_i \sin\phi_i \sin\kappa_i \\
m_{23} &= \sin\omega_i \cos\kappa_i + \cos\omega_i \sin\phi_i \sin\kappa_i \\
m_{31} &= \sin\phi_i \\
m_{32} &= -\sin\omega_i \cos\phi_i \\
m_{33} &= \cos\omega_i \cos\phi_i.
\end{aligned} \quad (2.23)$$

X_j, Y_j and Z_j are the object space coordinates of object point j; X_i^c, Y_i^c and Z_i^c are the object space coordinates of the exposure center of photo i; x_{ij} and y_{ij} are the image coordinates of object point j on photo i; f is the focal length of the camera; λ_{ij} is the photo scale factor at image point j in the newly rotated photo-coordi- about the $\bar{x}$-, $\bar{y}$- and $\bar{z}$-axis of the photo coordinate system.

The derivation to be presented in the following paragraphs will first assume that the photograph is parallel to the X-Y plane; *i.e.* $\omega_i = \phi_i = \kappa_i = 0$ as shown in figure 2-11. Then a small ω_i-rotation is introduced. It is followed by a small ϕ_i-rotation and a κ_i-rotation. This sequence of rotation is illustrated in fig. 2-12.

Let $\omega_i = \phi_i = \kappa_i = 0$, and let $\bar{x}_o$, $\bar{y}_o$ and $\bar{z}_o$ be the photo coordinates of image point j. It can be seen from figure 2-11 that the following relationships exist:

$$\begin{aligned}
X_j - X_i^c &= \lambda_{ij}\,\bar{x}_o \\
Y_j - Y_i^c &= \lambda_{ij}\,\bar{y}_o
\end{aligned} \quad (2.24)$$

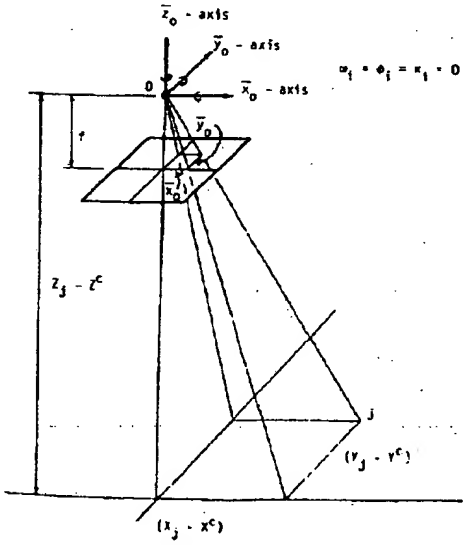

FIGURE 2-11. Zero-rotation case.

and

$$Z_j - Z_i^c = \lambda_{ij}\,\bar{z}_o.$$

Next, assume a small rotation ω_i and $\phi_i = \kappa_i = 0$. Let $\bar{x}_\omega$, $\bar{y}_\omega$ and $\bar{z}_\omega$ denote the coordinates of image point j in the newly rotated photo-coordinate system. It can be easily derived from figure 2-13a that

$$\begin{aligned}
\bar{x}_o &= \bar{x}_\omega \\
\bar{y}_o &= \bar{y}_\omega \cos\omega_i - \bar{z}_\omega \sin\omega_i \\
\bar{z}_o &= \bar{y}_\omega \sin\omega_i + \bar{z}_\omega \cos\omega_i.
\end{aligned}$$

Next introduce an additional rotation ϕ_i about the $\bar{y}_\omega$-axis as shown in figure 2-12b, and let $\bar{x}_{\omega\phi}$, $\bar{y}_{\omega\phi}$ and $\bar{z}_{\omega\phi}$ denote the coordinates of the same image point in the newly rotated system. The following equations can be derived from figure 2-13(b):

$$\begin{aligned}
\bar{x}_\omega &= \bar{x}_{\omega\phi} \cos\phi_i + \bar{z}_{\omega\phi} \sin\phi_i \\
\bar{y}_\omega &= \bar{y}_{\omega\phi} \\
\bar{z}_\omega &= -\bar{x}_{\omega\phi} \sin\phi_i + \bar{z}_{\omega\phi} \cos\phi_i.
\end{aligned} \quad (2.26)$$

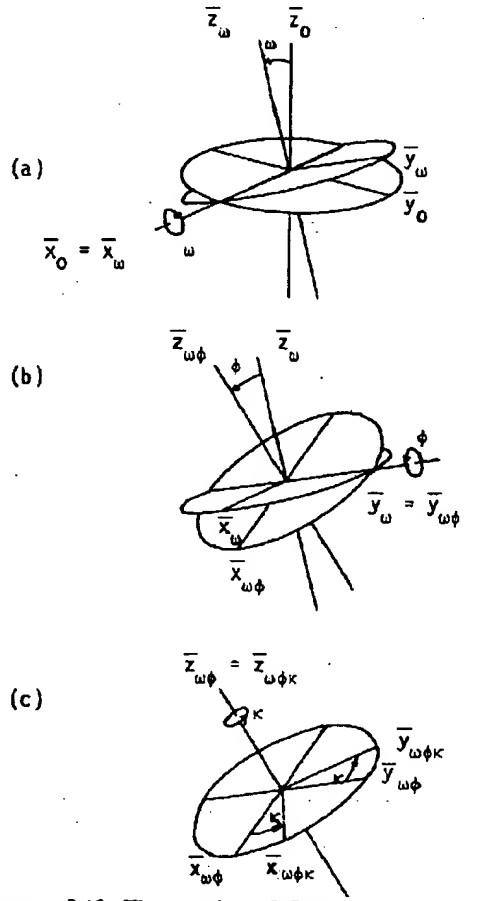

FIGURE 2-12. The rotations defined by the ω-ϕ-κ sequence.

Substituting equations (2.26) into equations (2.25) yields

$$\begin{aligned}\bar{x}_o &= \bar{x}_{\omega\phi} \cos\phi_i + \bar{z}_{\omega\phi} \sin\phi_i \\ \bar{y}_o &= \bar{x}_{\omega\phi} \sin\phi_i \sin\omega_i + \bar{y}_{\omega\phi} \cos\omega_i \\ &\quad - \bar{z}_{\omega\phi} \cos\phi_i \sin\omega_i \end{aligned} \tag{2.27}$$

and

$$\begin{aligned}\bar{z}_o &= -\bar{x}_{\omega\phi} \sin\phi_i \cos\omega_i + \bar{y}_{\omega\phi} \sin\omega_i \\ &\quad + \bar{z}_{\omega\phi} \cos\phi \cos\omega.\end{aligned}$$

Finally, introduce a κ-rotation about the $\bar{z}_{\omega\phi}$-axis as shown in figure 2-12c, and let $\bar{x}_{\omega\phi\kappa}$, $\bar{y}_{\omega\phi\kappa}$ and $\bar{z}_{\omega\phi\kappa}$ denote the coordinates of the image point in the newly rotated system. The following equations can be derived from figure 2-13c:

$$\begin{aligned}\bar{x}_{\omega\phi} &= \bar{x}_{\omega\phi\kappa} \cos\kappa_i - \bar{y}_{\omega\phi\kappa} \sin\kappa_i \\ \bar{y}_{\omega\phi} &= \bar{x}_{\omega\phi\kappa} \sin\kappa_i + \bar{y}_{\omega\phi\kappa} \cos\kappa_i \end{aligned} \tag{2.28}$$

and

$$\bar{z}_{\omega\phi} = \bar{z}_{\omega\phi\kappa}.$$

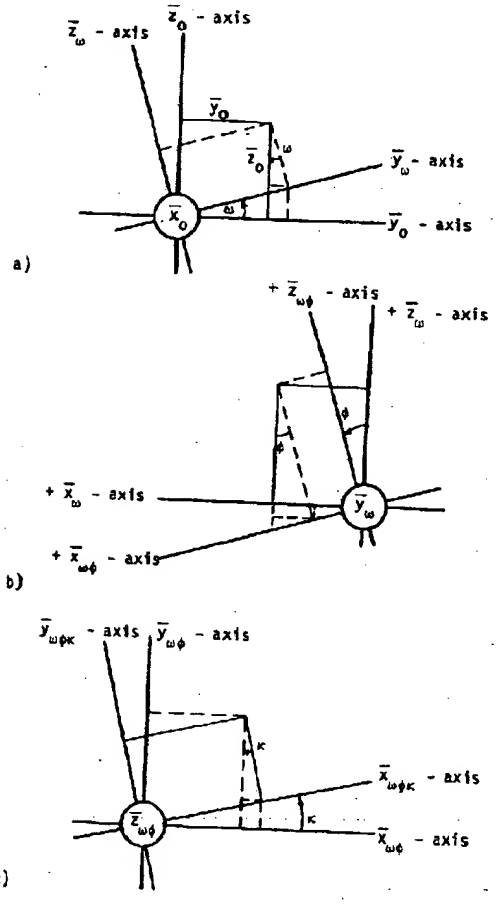

FIGURE 2-13. Plane cross-sections about axis of rotation.

Substituting these equations into equations (2.27) yeilds

$$\begin{aligned}\bar{x}_o &= \bar{x}_{\omega\phi\kappa} \cos\phi_i \cos\kappa_i - \bar{y}_{\omega\phi\kappa} \sin\kappa_i \cos\phi_i \\ &\quad + \bar{z}_{\omega\phi\kappa} \sin\phi_i \\ \bar{y}_o &= \bar{x}_{\omega\phi\kappa} (\cos\kappa_i \sin\phi_i \sin\omega_i + \sin\kappa_i \cos\omega_i) \\ &\quad + \bar{y}_{\omega\phi\kappa} (\cos\kappa_i \cos\omega_i - \sin\kappa_i \sin\phi_i \sin\omega_i) \\ &\quad - \bar{z}_{\omega\phi\kappa} (\cos\phi_i \sin\omega_i) \end{aligned} \tag{2.29}$$

and

$$\begin{aligned}\bar{z}_o &= \bar{x}_{\omega\phi\kappa} (\sin\kappa_i \sin\omega_i - \cos\kappa_i \sin\phi_i \cos\omega_i) \\ &\quad + \bar{y}_{\omega\phi\kappa} (\sin\kappa_i \sin\phi_i \cos\omega_i + \sin\kappa_i \cos\kappa_i) \\ &\quad + \bar{z}_{\omega\phi\kappa} (\cos\phi_i \cos\omega_i).\end{aligned}$$

In equations (2.29), $\bar{x}_{\omega\phi\kappa}$, $\bar{y}_{\omega\phi\kappa}$ and $\bar{z}_{\omega\phi\kappa}$ denote the photo-coordinates of an image point on a tilted photograph. Since in practice all aerial photographs can be assumed to have some small tilt, the subscripts for these coordinates can be dropped without any los of generality; that is,

$$\begin{aligned}\bar{x}_j &= \bar{x}_{\omega\phi\kappa} = x_j - x_p \\ \bar{y}_j &= \bar{y}_{\omega\phi\kappa} = y_j - y_p \\ \bar{z}_j &= \bar{z}_{\omega\phi\kappa} = -f.\end{aligned} \tag{2.30}$$

Substituting equations (2.30) into (2.29) and then substituting the resulting equations into (2.24) will yield the projective transformation equation (2.22) which is stated at the beginning of this section.

It is recalled that the following assumptions were made in the above derivation: (1) the image (x, y, z) and object (X, Y, Z) coordinate systems are both right-handed; (2) the sequence of angular rotations is ω, ϕ, κ, where ω is the first rotation and is about the X axis; (3) the x, y, z coordinates refer to a contact print of a photograph (diapositive with emulsion upward); and (4) one visualizes a vertical or near-vertical photograph as though looking downward from an airplane. But one is reminded that these assumptions do not always apply: (1) in certain European systems the geodetic rectangular coordinate system is different; (2) ω need not be the first of the sequence of rotations; (3) where glass plates are used in a camera, measurements are usually made on the original negative instead of the diapositive, and if aerotriangulation is being performed for the eventual use of a compilation instrument like the Kelsh plotter, the diapositives may be printed through the film base and the emulsions are not in contact; (4) for horizontal (terrestrial) photographs certain terms are already defined by convention and for astronomical work the camera "looks" upward instead of downward; and (5) the measuring comparator may impose arbitrary considerations with regard to the designation of the x and y axes and the plus and minus directions (Rosenfield 1959).

The subject of coordination of the various rotational systems was the basis for a resolution

adopted by the International Congress on Photogrammetry which met in Stockholm in 1956. The ideas of the resolution are expressed by Schermerhorn (1955).

The right-handed system adopted has the Z axis downward and the X axis to the right; the position of the Y axis is thus predetermined. The Stockholm system is equivalent to the geodetic coordinate system of many European countries: X north, Y east, and Z downward.

In the United States, the geodetic coordinate system upon which surveying and mapping is based regards the Z axis as upward, the X axis to the East, and Y axis to the North. This is also a right-handed system. Again, in this country, the survey (azimuth) and navigation angles are measured clockwise for the positive direction. Thus, the basis for the recommendation of the Stockholm resolution can be adopted in this country by assuming a photogrammetric system based on our geodetic system.

It is readily seen that the two systems are the same in abstract space and the formula for any rotation about a given axis in either system would therefore be the same.

2.2.3.2.4 Tilt, Swing and Azimuth

The orientation of a photograph can also be defined by the three rotation angles tilt (t), swing (S) and azimuth (α), which are illustrated in figure 2-14. The tilt angle (t) is measured in the principle plane from the optical axis of the camera to the plumb line and always has a positive sign. The direction of tilt with respect to the photographic axes is defined by the swing angle (S), which is measured clockwise from the positive y-axis of the photograph to the lower part of the principal line which passes through the nadir point (n). The direction of tilt with respect to the ground reference coordinate system (X, Y, Z) is defined by the azimuth angle (α), which is measured in the X-Y plane clockwise from the positive Y axis to the projection of the principal line on the X-Y plane.

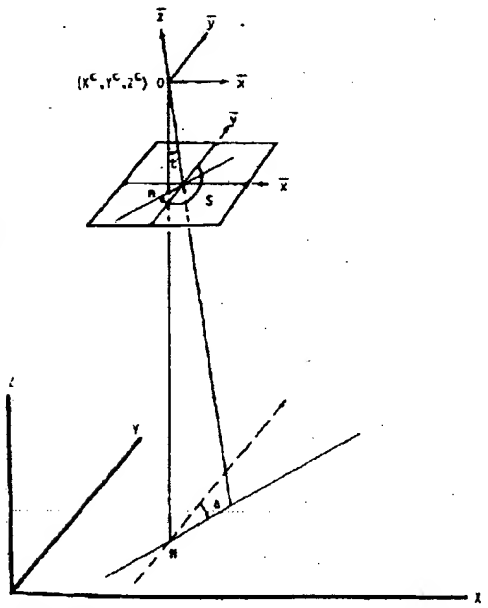

FIGURE 2-14. Rotation angles tilt (±), swing (S) and azimuth (α).

The elements m_{ij}'s in projective transformation equations (2.22) may be expressed in terms of t, S and α as follows:

$$
\begin{aligned}
m_{11} &= -\cos S \cos \alpha - \sin S \cos t \sin \alpha \\
m_{12} &= \sin S \cos \alpha - \cos S \cos t \sin \alpha \\
m_{13} &= -\sin \alpha \sin t \\
m_{21} &= \cos S \sin \alpha - \sin S \cos t \cos \alpha \\
m_{22} &= -\sin S \sin \alpha - \cos S \cos t \cos \alpha \\
m_{23} &= -\cos \alpha \sin t \\
m_{31} &= -\sin S \sin t \\
m_{32} &= -\cos S \sin t \\
m_{33} &= \cos t.
\end{aligned} \tag{2.31}
$$

A major disadvantage of this system of defining orientation is that it breaks down for the ideal aerial photograph which is truly vertical. When there is no tilt, the two planes are either parallel or coincident, and there is no line of intersection (or principal line); thus, the angles of swing and azimuth are undefined.

2.2.3.2.5 Terrestrial Photogrammetry

In terrestrial photogrammetry, the orientation of the photograph can often be more conveniently described by the three rotation angles *omega* (ω), *alpha* (α), and *kappa* (κ) which are illustrated in figure 2-15. *Omega* is a rotation about the $\bar{x}$-axis of the photo-coordinate system and is measured positive in the counter-clockwise direction. *Alpha* (α) is a rotation about the $\bar{y}$-axis of the photo-coordinate system and is measured positive in the *clockwise* direction. *Kappa* (κ) is a rotation about the $\bar{z}$-axis and is measured positive in the counter-clockwise direction. When $\omega = \alpha = \kappa = 0$, the $\bar{x} - \bar{z}$ plane is parallel to the $X - Y$ plane and the $\bar{z}$-axis is parallel to the Y-axis but points in the opposite direction. The ground coordinate system is commonly defined so that the Z-axis is the local vertical and the Y-axis points in the direction of true north. Then, the *alpha* (α) angle is the horizontal azimuth of the optical axis measured clockwise from true north; and the *omega* (ω) angle measures the tilt angle of the optical axis with respect to the horizontal plane.

The elements m_{ij}'s in projective transformation equations (2.22) may be expressed in terms of ω, α and κ as follows:

$$
\begin{aligned}
m_{11} &= \cos \alpha \cos \kappa \\
m_{12} &= -\sin \omega \sin \kappa - \cos \omega \sin \alpha \cos \kappa
\end{aligned}
$$

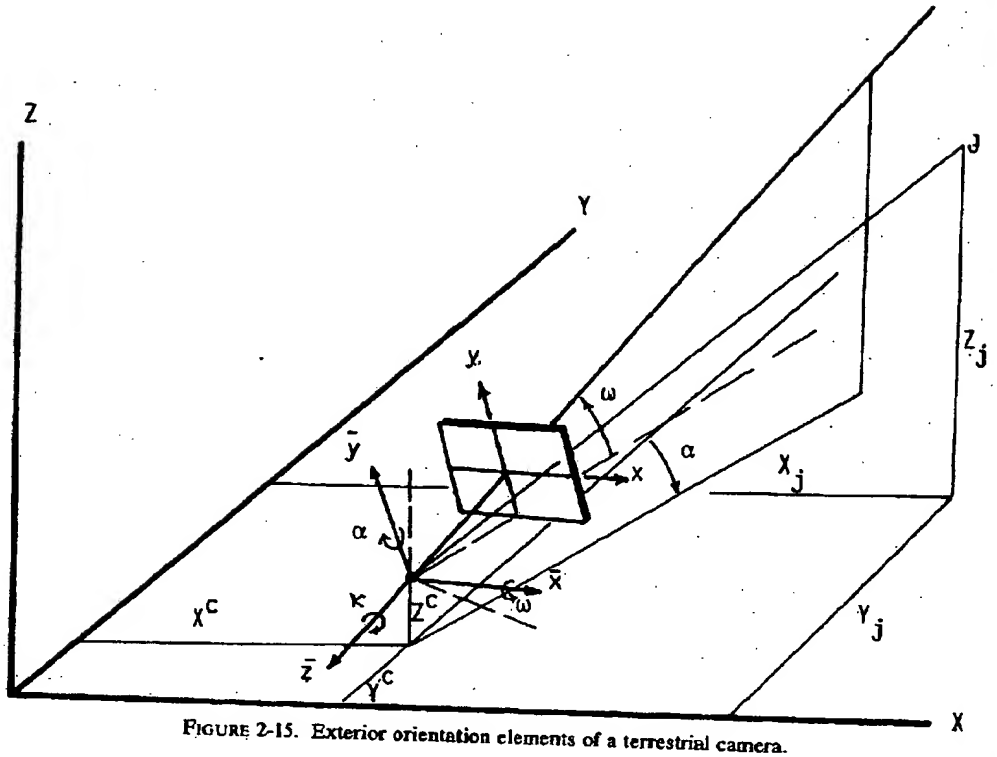

FIGURE 2-15. Exterior orientation elements of a terrestrial camera.

$$
\begin{aligned}
m_{13} &= \cos\omega \sin\kappa - \sin\omega \sin\alpha \cos\kappa \\
m_{21} &= -\cos\alpha \sin\kappa \\
m_{22} &= -\sin\omega \cos\kappa + \cos\omega \sin\alpha \sin\kappa \\
m_{23} &= \cos\omega \cos\kappa + \sin\omega \sin\alpha \sin\kappa \\
m_{31} &= -\sin\alpha \\
m_{32} &= -\cos\omega \cos\alpha \\
m_{33} &= -\sin\omega \cos\alpha.
\end{aligned} \tag{2.32}
$$

The sequence of rotations used in deriving the above expressions is as follows: ω-rotation first, α-rotation second, and κ-rotation last.

2.2.3.3 Relative Orientation

Relative orientation is the determination of the relative position and attitude of the two photographs in a stereoscopic pair with respect to each other. The primary purpose of relative orientation is to orient the two photographs so that each corresponding pair of rays from the two photographs intersect in space. This condition is achieved at the completion of relative operation only if the optical lens system in both the camera and the projector of the stereoplotter are distortionless, if the light rays truly travel in straight lines through the atmosphere, and if no geometric distortion is introduced into the photographic image during the photographic processing. These conditions are rarely satisfied in practice, and usually the corresponding pair of rays from the two photographs cannot be all made to intersect exactly in space. The objective of relative orientation is then to orient the two photographs so that the condition of intersection is as nearly achieved as possible.

2.2.3.3.1 Geometric Conditions for Relative Orientation

Assuming the absence of geometric distortions caused by various sources, the relative orientation of a stereoscopic pair of photographs is accomplished by making five pairs of rays intersect. That is, if five pairs of rays intersect, then every pair of rays in the two bundles will intersect. Figure 2-16 shows the general location of the six pairs of rays that are universally used for performing relative orientation in a stereoplotter. Five of the six pairs are absolutely needed for performing relative orientation, and the sixth pair is used for checking purposes. This geometric condition will become obvious from examination of the coplanarity equation which will be derived in section 2.2.3.3.3.

2.2.3.3.2 Mathematical Definition

Let X_L, Y_L and Z_L be the object space coordinates of the exposure center and ω_L, ϕ_L and κ_L be the rotation angles of the left photograph. These six parameters then define the exterior orientation of the left photograph. Similarly, let X_R, Y_R, Z_R, ω_R, ϕ_R and κ_R be the exterior orientation parameters of the right photograph.

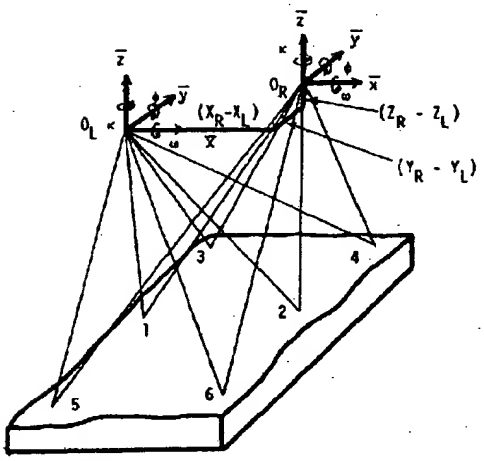

FIGURE 2-16. Geometric conditions for relative orientation.

Then mathematically speaking, a stereoscopic pair of photographs is said to be relatively oriented with respect to each other if the following five parameters are known: $(Y_R - Y_L)$, $(Z_R - Z_L)$, $(\omega_R - \omega_L)$, $(\phi_R - \phi_L)$, $(\kappa_R - \kappa_L)$. These parameters are illustrated in figure 2-16. It is assumed here that the X-axis is approximately along the direction of flight. The separation of the two photographs along the X-direction, $X_R - X_L$, controls the scale of the model and is not a parameter of relative orientation.

2.2.3.3.3 Coplanarity Equation

In figure 2-17, $\bar{A}_i$ denotes the vector which originates from the exposure center (O_i) of the left photo, passes through image point a_i, and ends at point a in the object space. Similarly, $\bar{A}_j$ denotes the vector from the right exposure center (O_j) to the same point a. The vector $\bar{B}$ extends from O_i to O_j. Then, the conditions that the two vectors, $\bar{A}_i$ and $\bar{A}_j$, intersect in space is expressed by the following equation:

$$(\bar{A}_i \times \bar{A}_j) \cdot \bar{B} = 0. \tag{2.33}$$

From figure 2.17, the vector $\bar{A}_i$ may be expressed in terms of its components as follows:

$$\bar{A}_i = (X_a - X_i^c)\,\bar{i} + (Y_a - Y_i^c)\,\bar{j} + (Z_a - Z_i^c)\,\bar{k}. \tag{2.34}$$

From the projective transformation equation (2.22),

$$\begin{aligned} X_a - X_i^c &= \lambda_i [m_{11}(x_i - x_p) + m_{21}(y_i - y_p) + m_{31}(-f)] \\ Y_a - Y_i^c &= \lambda_i [m_{12}(x_i - x_p) + m_{22}(y_i - y_p) + m_{32}(-f)] \end{aligned} \tag{2.35}$$

and

$$Z_a - Z_i^c = \lambda_i [m_{13}(x_i - x_p) + m_{23}(y_i - y_p) + m_{33}(-f)]$$

where the m_{ij}'s are functions of the rotation angles ω_i, ϕ_i and κ_i of photo i; x_p and y_p are photo-coordinates of the principal point; x_i and y_i are photo-coordinates of the image point a_i; and λ_i is a scale factor.

Let

$$\begin{aligned} u_i &= m_{11}(x_i - x_p) + m_{21}(y_i - y_p) + m_{31}(-f); \\ v_i &= m_{12}(x_i - x_p) + m_{22}(y_i - y_p) + m_{32}(-f); \end{aligned} \tag{2.36}$$

and

$$w_i = m_{13}(x_i - x_p) + m_{23}(y_i - y_p) + m_{33}(-f).$$

Then Equation (2.35) may be written as

$$\begin{aligned} X_a - X_i^c &= \lambda_i u_i \\ Y_a - Y_i^c &= \lambda_i v_i \end{aligned} \tag{2.37}$$

and

$$Z_a - Z_i^c = \lambda_i w_i.$$

Substituting Equation (2.37) into (2.34) yields

$$\bar{A}_i = \lambda_i u_i \bar{i} + \lambda_i v_i \bar{j} + \lambda_i w_i \bar{k}. \tag{2.38}$$

A similar equation can be derived for the vector $\bar{A}_j$ from the right photograph:

$$\bar{A}_j = \lambda_j u_j \bar{i} + \lambda_j v_j \bar{j} + \lambda_j w_j \bar{k}. \tag{2.39}$$

Furthermore, the following expression for vector $\bar{B}$ can be derived directly from figure 2.17:

$$\bar{B} = (X_j^c - X_i^c)\,\bar{i} + (Y_j^c - Y_i^c)\,\bar{j} + (Z_j^c - Z_i^c)\,\bar{k}. \tag{2.40}$$

The coplanarity condition stated in equation (2.33) is then satisfied if the determinant

$$\begin{vmatrix} (X_j^c - X_i^c) & (Y_j^c - Y_i^c) & (Z_j^c - Z_i^c) \\ u_i & v_i & w_i \\ u_j & v_j & w_j \end{vmatrix} = 0 \tag{2.41}$$

That is,

$$\begin{aligned} (X_j^c - X_i^c)(v_i w_j - v_j w_i) + (Y_j^c - Y_i^c)(u_j w_i - u_i w_j) \\ + (Z_j^c - Z_i^c)(u_i v_j - u_j v_i) = 0 \end{aligned} \tag{2.42}$$

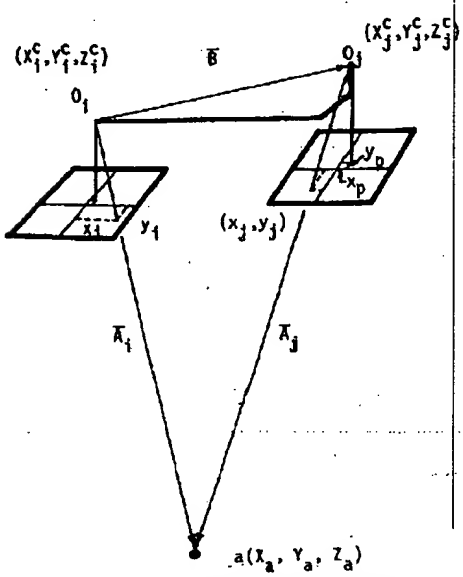

FIGURE 2-17. Condition of coplanarity.

which is commonly known as the coplanarity equation. There are twelve parameters in the equation: X_l^c, Y_l^c, Z_l^c, ω_l, ϕ_l, κ_l, X_j^c, Y_j^c, Z_j^c, ω_j, ϕ_j and κ_j. The problem of relative orientation only requires the solution of the five differential parameters $(Y_j^c - Y_l^c)$, $(Z_j^c - Z_l^c)$, $(\omega_j - \omega_l)$, $(\phi_j - \phi_l)$ and $(\kappa_j - \kappa_l)$. Therefore, arbitrary values can be assigned to the parameters X_l^c, Y_l^c, Z_l^c, ω_l, ϕ_l, κ_l and X_j^c, and then the only unknowns to be solved in a relative orientation problem will be Y_j^c, Z_j^c, ω_j, ϕ_j and κ_j. Each pair of rays for which the image coordinates x_l, y_l, x_j and y_j have been measured gives rise to one coplanarity equation. Thus five pairs of rays would yield five equations which are the minimum required to solve for the five unknowns of relative orientation. Of course, equation (2.42) is non-linear and must first be linearized before it can be used for solution. In addition, when more than five pairs of image coordinates are measured, the method of least squares may be used to determine the most probable solution. The methods of linearization of equations and least squares will be discussed in section 2.5.

2.2.3.4 Absolute Orientation

After relative orientation is accomplished, the stereo model must be scaled, translated and leveled with respect to a ground reference coordinate system. The process of orienting a stereo-model into an absolute reference system is called absolute orientation. Mathematically, the problem may be defined simply as a problem of coordinate transformation. Referring to figure 2-18, let x_j, y_j and z_j represent the coordinates

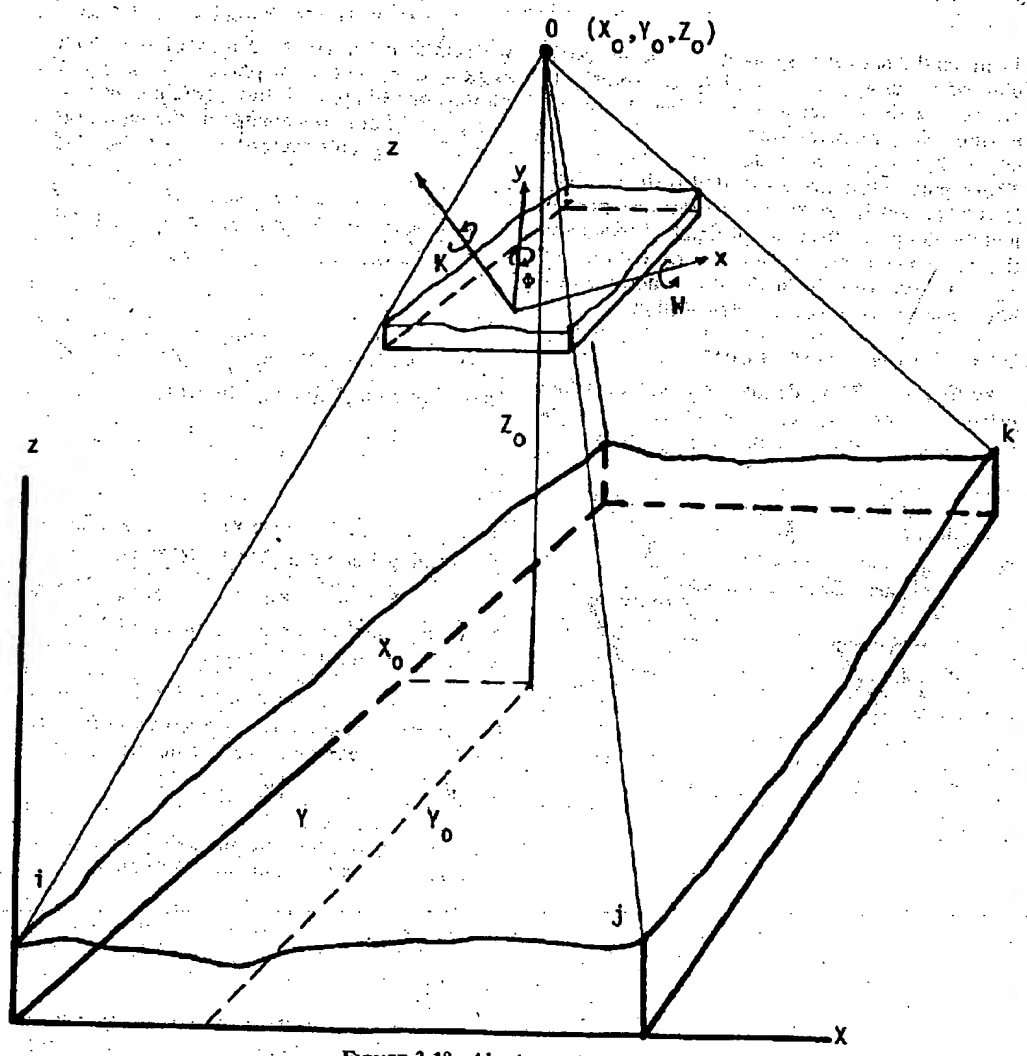

Figure 2-18. Absolute orientation.

of point j in the model coordinate system, and let X_j, Y_j and Z_j be the coordinates of the same point in the ground reference system. Then the relationship between the model coordinates (x_j, y_j and z_j) and the ground coordinates (X_j, Y_j and Z_j) may be expressed by the projective transformation equations derived in section 2.2.3.2.3; *i.e.*

$$\begin{aligned} X_j - X_o &= \lambda \left[m_{11} x_j + m_{21} y_j + m_{31} z_j\right] \\ Y_j - Y_o &= \lambda \left[m_{12} x_j + m_{22} y_j + m_{32} z_j\right] \\ Z_j - Z_o &= \lambda \left[m_{13} x_j + m_{23} y_j + m_{33} z_j\right] \end{aligned} \tag{2.43}$$

in which

$$\begin{aligned} m_{11} &= \cos \Phi \cos K \\ m_{12} &= \cos W \sin K + \sin W \sin \Phi \cos K \\ m_{13} &= \sin W \sin K - \cos W \sin \Phi \cos K \\ m_{21} &= -\cos \Phi \sin K \\ m_{23} &= \cos W \cos K - \sin W \sin \Phi \sin K \\ m_{23} &= \sin W \cos K + \cos W \sin \Phi \sin K \\ m_{31} &= \sin \Phi \\ m_{32} &= -\sin W \cos \Phi \\ m_{33} &= \cos W \cos \Phi. \end{aligned} \tag{2.44}$$

The transformation parameters include a scale factor (λ), three translation parameters (X_o, Y_o, and Z_o) and three rotation parameters (W, Φ and K). Each control point, for which the ground coordinates are known, gives rise to three equations when its model coordinates are measured. Thus, a minimum of three control points in the model area will be needed to perform the absolute orientation. Again, equation (2.43) must be linearized before it can be used in the solution for the absolute orientation parameters and the method of least squares may also be used.

The procedure for performing absolute orientation in a stereoplotter will be discussed in chapters XI and XII.

2.2.4 GEOMETRICAL SOLUTIONS TO SOME PHOTOGRAMMETRIC PROBLEMS

Photogrammetric methods are commonly used to map the topography of the terrain, size and shape of objects as well as the precise location of discrete points in an object space. The accuracy and precision of the measurements depend on the quality of the hardware and software used in both data collection (such as photography) and data reduction. Photogrammetric cameras of outstanding geometric fidelity have been developed for both aerial and terrestrial mapping projects. Mono- and stereocomparators having a precision in the order of 1 μm are commonly available, and rigorous computer softwares have been developed for analytical aerotriangulation yielding a precision approaching that of first-order geodetic surveys. Fully automated stereoplotting instruments of high precision have been used in routine production for many years. Detailed dicussions on these hardwares and softwares will be presented in later chapters in this manual. It will suffice to state here that the types of instruments and the data reduction procedures to be used in a given project situation depends largely on the accuracy that is required. This section will present a few computational methods that are derived from simple geometric principles and which have been commonly used in applications where high-order of accuracy of measurement is not required.

2.2.4.1 Stereoscopic Parallax and Elevations

The stereoscopic parallax of a point A which is imaged in the overlap area of a stereoscopic pair of photographs is defined as the difference in the x-components of distances in the two photographs which are measured from the principal point to the image point A. Because stereoscopic parallax is measured along the x-axis which is in the direction of flight of the aircraft, it is commonly referred to as x-parallax. In a given pair of vertical aerial photographs, the difference in parallax or parallax difference between two image points is directly related to the difference in elevations of the two points on the ground.

In figure 2-19, two truly vertical photographs of equal focal length f are shown a distance $OO' = B$ apart and at an altitude H above a horizontal reference plane. An object A has an elevation h and images of A occur at a on the left photograph and at a' on the right one. An x axis is adopted on each photograph parallel to OO', and n and n' are both the principal points and nadir points of the respective photographs. The ordinates aa_1 and $a'a_1'$ are perpendicular to the x axis. Triangle $OO'A_1$ is in the vertical plane that contains the two perspective centers (camera stations), AA_1 is perpendicular to plane $OO'A_1$, and the elevation of A_1 is also h. The absolute stereoscopic parallax of A is defined as the algebraic difference of the absissas na_1 and $n'a_1'$:

$$p = x - x'.$$

The parameters in the above equation are illustrated graphically in the smaller figure which is composed of triangle Oa_1n of the left photograph and triangle $O'a_1'n'$ of the right one. It can be shown by similar triangles that

$$\frac{p}{f} = \frac{B}{H - h} \tag{2.45}$$

$$h = H - \frac{Bf}{p}. \tag{2.46}$$

It is to be noted that the derivation of these equations is based on (1) utilted photographs,

TABLE 4-3.—AERIAL CAMERAS

Camera Type	Use	Basic Design	Cycling Time	Focal Length	Lens Apert.	Format Size	Shutter Type	Shutter Speed (sec.)	Weight (lbs.)	Film Mag.	Film Size
KA-63A	Day vert. Day twin Night vert	Frame	3 sec per cycle	58 mm 80 mm 6"	f/4.5 f/5.6 f/2.8	2.25" × 9.45" 2.25" × 9.45" 2.25" × 4.5"	D-f. plane N-self Capping	1/500–1/1,000 or 1/2,000 Man. Set	60	LA/364A Cassette	9½"
KA/68A	Day Recon	Panoram.	1 to 6 per second	3" Biogon	f/4.5	4.5" × 9.4"	Var. Slit at F. plane	1/92.5–1/5,000	90	Cassette	5"
KA-74A	Day Recon Night Recon	Frame	1, 2 or 4 f/s 1 or 2 f/s	6"	f/2.8	4.5" × 4.5"	Focal Plane	1/1,000, 1/2,000	37	LA-384A	5"
KA-76A	Day-Night Recon	Frame	6 per sec	6" 1.75" 3" 12"	f/2.8 f/5.6 f/4.5 f/3.5	4.5" × 4.5"	Focal Plane	1/60–1/3,000	52.5 51.75 58.25 68.5	LA-414A Cassette	5"
KA-82A	Day Recon	Panoram	10 sec/cycle to 1.17 c/s, autocy.	12"	f/3.8	4.5" × 29.3"	Focal Plane	1/30–1/12,000	216.7	LA/418A Cassette	5"
KA-88A	Day Recon	Frame	2 sec max	24"	f/8.0	9" × 9"	Focal Plane	1/500, 1/1,000 1/2,000	135	Cassette	9½"

are measured, and the data reduced from measurements provide the elements of interior orientation. Many physical controls are essential.

(2) To clamp a master grid at the focal plane and to measure the observed angles in object space, a visual or photogoniometer technique. The distortion is computed from the focal length and the difference between the image and object angles.

Whichever of the many variations of these two methods is employed, the physicist is concerned with the design, maintenance, and accuracy of sensitive precision equipment and the use of evaluation techniques which are substantially free of error.

The calibrated values and their accuracy are then reported in a camera calibration certificate with tables and graphs.

4.8.1.1 DEFINITIONS

In accordance with recommendations from the International Society of Photogrammetry (ISP), the word "measured" is being used to stop the confusion between image position error, as found in practice, and distortion, the aberration calculated by the lens designer. The latter is always symmetrical and has no tangential component. The ISP recommends use of the word "best" in principal point of best symmetry to emphasize that perfect symmetry is not obtainable, and further that choice of the point depends on the interpretation of "best."

All characteristics that affect the geometry of the photograph are calibrated. These are here termed elements of interior orientation (*see* also chapter II), and, depending on the quality of the camera, may include the following: (*see* figure 4-45).

a. Equivalent Focal length (EFL)

$$\text{EFL} = \frac{d\alpha}{\tan \alpha} \tag{4.19}$$

with the reasonable assumption that there is no distortion at the small angles. $d\alpha$ is the average distance between the images of the center

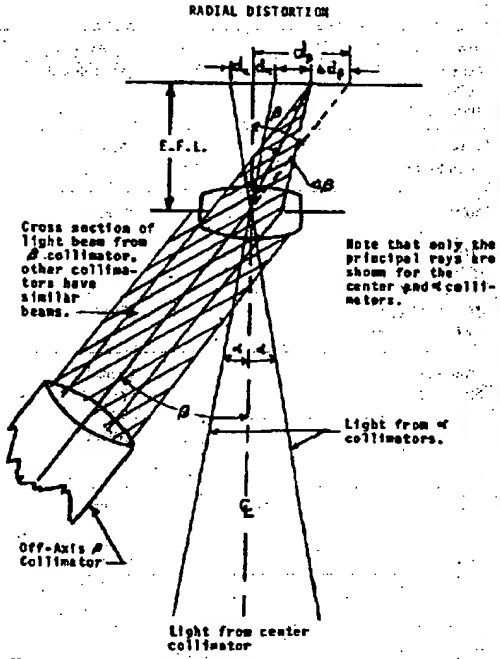

FIGURE 4-45. Effective focal length and radial distortion. This drawing explains the geometry. Using known angles in object space, usually 7.5° or less, and the measured distance between the images, the effective focal length is a computed value. Δd_β is the radial distortion.

IN CURRENT USE (1978)—Continued

Film Load	Film Spools Core Dia.	Film Spools Flange Dia.	Mount Used	Status	Mfr's Name	General Remarks	Camera Type
180'	75' spool–MS26565-15 200'–spool–MS26565-17		Fixed	Std.	Chicago Aerial Ind	Hor. to hor. day or night vert.; Army	KA-63A
1000' Thin base			Fixed		Fairchild	Low alt hor. to hor.; rotating double dove prism	KA-68A
100' (5.2 mil) 180' (2.5 mil)			LA-366A	Std.	Actron	Vert fwd rt and left obl; part of KS-91A Surv sys	KA-74A
250'	MS-26565-9		LA-408A LA-409A LA-160A	Std.	Chicago Aerial Ind	Part of KS-104A & B photo sys in Army OV-1 ac	KA-76A
2000'			Shock mount	Std.	Fairchild	Med or high alt.; rotary lens	KA-82A
1500' thin base			3 pt vib isol fixed V/H rocking		Actron	Med to high alt.; nodding five position; HC-338A	KA-88A

target and that of a small off-axis image, usually 7.5° or less for a wide-angle mapping lens. α is the angle in object space.

b. Average Radial Measured Distortion: When the incident ray from an off-axis object is deviated while traversing the lens so that the distance d_s between the center and off-axis images, $d_s \neq$ EFL tan B, but

$$d_s = \text{EFL} \tan B \pm \Delta d_s \qquad (4.20)$$

then Δd_s is the radial distortion, being negative when the image distance is less then EFL tan B and positive when greater. When there are several images for similar angular targets, they are averaged. Distortion is plotted in micrometres as a function of image distance in millimetres, or in micrometres as a function of angle (figure 4-46).

c. Asymmetrical Radial Measured Distortion is the variation from the average value.

d. Calibrated Focal Length (CFL)

$$\text{CFL} = \text{EFL} \pm \Delta f \qquad (4.21)$$

When the EFL is adjusted by adding or subtracting Δf to EFL, to provide a preferred balance of the measured distortion curve, usually balancing positive and negative peaks or obtaining a least squares balance, the adjusted value is termed the calibrated focal length and is used in optical projection systems and/or for mathematical corrections.

e. Tangential Measured Distortion is a displacement of the image perpendicular to a straight radial line from the lens axis, and, similarly to radial distortion, is measured in the image plane. It is a manufacturing error which can be minimized by precise centering of lens elements and their selected azimuth rotations.

f. Principal Point of Best Symmetry (see second edition "MANUAL OF PHOTOGRAMMETRY," Camera Calibration, Sewell). A point is selected which reduces the asymmetry of the distortion to a minimum.

g. Fiducial Center or Indicated Principal Point (IPP). If imaginary lines are drawn between opposite fiducials as between A and B and its approximately perpendicular pair C and D, the crossing of the imaginary lines defines the fiducial center, also termed the Indicated Principal Point. A different design features corner fiducials such as E-F and G-H. Fiducials must be small and clearly defined so that the center can be located within a few micrometres. Note that there is no agreement on labeling fiducials (figure 4-47).

h. Angle between the theoretical lines drawn between opposite fiducials: This angle is measured during the calibration tests and is usually required to deviate less than one-minute-of-arc from 90°.

i. Distance between opposite fiducials: In the photographic techniques of camera calibration, the fiducials are recorded on rigid emulsion-coated glass plates when these plates are exposed in the focal plane of the camera. The measured distances (A to B and C to D; or E to F and G to H; or both) are reported in the calibration certificate.

j. Principal Point of Autocollimation (PPA). The PPA is the location at which the image of the zero degree collimator target is recorded when the focal plane of the camera is positioned precisely perpendicular to the direct ray from that target. The location of the PPA is referenced to the IPP.

k. Coordinate System of Fiducials: When the positions of the fiducials are reported with respect to a coordinate system, the geometry provides a better control. In one such case, the fiducial center becomes the origin, the A-B line being coincident with the x-axis. A theoretical line perpendicular to the x-axis and intersecting the IPP is then the y-axis. The remaining fiducials are referenced to this coordinate system. Other arrangements are also used.

l. Vacuum Platen Contour. When the mapping camera is equipped with vacuum to hold the

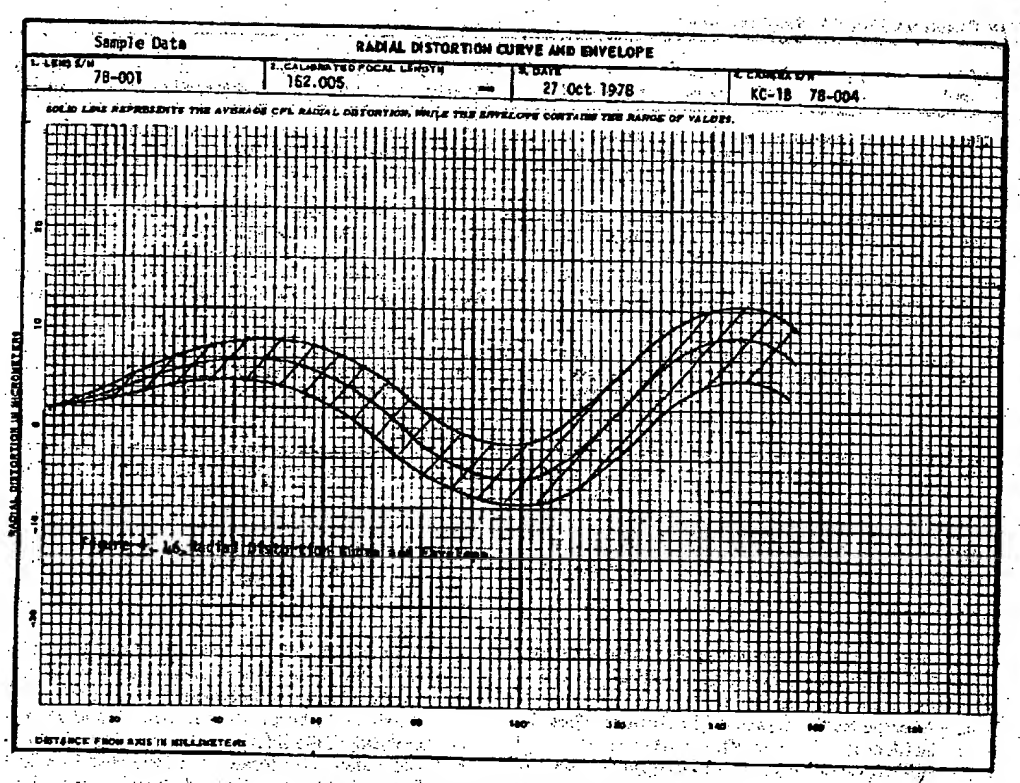

FIGURE 4-46. Radial distortion curve and envelope.

film in contact with the magazine platen during exposure, it is necessary that the contour of the platen follow the intended focal plane of the lens so that distortion is not introduced into the photograph. In most cases, the focal plane of the lens is flat and measurements of the platen are made to show significant deviations. Users can then choose to correct these biases mathematically.

m. Reseau Measurements. There are various patterns of reseau which are recorded as points or crosses on the film during exposure. Their primary purpose is to provide control for film dimensions. When the reseau is fixed with respect to the lens, it may also substitute for the fiducials, certain reseau marks being selected from which to locate the fiducial center, the line of flight, the point of best symmetry, and other control points. Reseau points should be measured directly or from recordings on emulsion-coated plates positioned at the focal plane to assure accuracy.

n. Resolution and Optical Transfer Functions. These are the two best known and most used criteria of image quality. A static test will show the quality of the focus while a dynamic test, camera and magazine operational, will show the quality of focus in conjunction with the film handling characteristics, a measure of operational image quality. Either test may be reported in the camera calibration certificate.

o. Radial Distortion Polynomial. A polynomial of three or four terms may be determined using the measured values of average radial distortion. This is reported in the form:

$$\Delta r = ar + br^3 + cr^5 + dr^7 + \ldots \quad (4.22)$$

Where the r's are average radial image distances in millimetres and Δr is in micrometres.

Note that this equation is anti-symmetrical and gives best results when referenced to the Point of Best Symmetry. If applied with reference to the Principal Point of Autocollimation, the asymmetries will be larger in accordance as the distance between the two points increases.

p. Tangential Distortion Polynomial. A two- or three-term polynomial for tangential distortion may also be derived, but symmetry exists only along each separate diagonal of the format. Along this diagonal the distortion increases with the distance from the center. This is not an aberration peculiar to design, but the result of decentering of the optical elements of which the lens is composed. It is possible for a camera to acquire tangential distortion if a perfect lens is subject to small lateral forces which disturb the collinearity of the elements. Theoretically, there is a diameter of the focal plane along which the tangential distortion is zero, and the diameter perpendicular to it along which the distortion is maximum.

When cameras are calibrated on a multicollimator, the tangential distortion can be measured directly along any diagonal. The

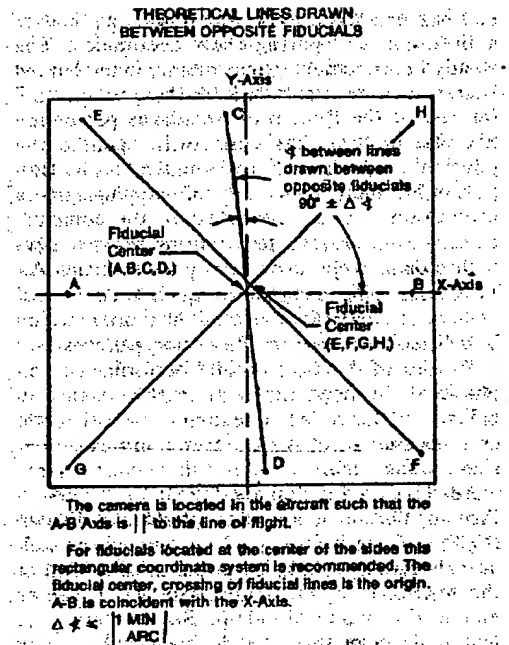

FIGURE 4-47. Fiducial center or indicated principal point. A rectangular coordinate system.

maximum radius vector can then be computed from the data from the two diagonals. Washer (1957) employed asymmetric radial measurements when he investigated tangential distortion. Using a thin prism as a model, he computed the position of a principal point and the wedge angle of the prism. This was reported in the Bureau of Standards Camera Calibration Certificate for many years, during which time manufacturers of cartographic lenses developed techniques which greatly reduced this centering error.

Brown also investigated this error, returning to the early writings of Conrady (1919). The equations he uses are applicable to all types of camera calibration and are given in section 4.8.8.2.

4.8.1.2 Calibration of Comparators

Measurements of images on spectroscopic plates or film are usually made with a two-coordinate comparator. A master grid which approximately equals the working area of the two ways is then employed to calibrate the comparator. The area of the master grid should be larger than the 23 cm × 23 cm square platens of the majority of mapping cameras employed. The standard should also provide means of measuring the orthogonality of the ways. An operator observes the grid points through the comparator microscope and selects the measuring value. The final values are compared with the standard.

Each laboratory has its preferred sequence of reading the coordinates of the grid, the number of repeated readings, and the reading pattern. Data are reduced, usually by iteration using a least squares program, until a best fit to the grid is obtained, or until a pattern of errors surfaces. Corrections can then be made either by adjusting the comparator or by correcting the measured numbers.

Temperature control of a comparator is essential in order to obtain reliable measurements. An example of such control is the constant bathing of the lead screw of a Mann comparator with cooled oil. The comparator remains accurate during long hours of use because the temperature is kept constant.

There are other types of visual comparators which do not employ screws but the same principles of calibration and environmental control apply.

Some automatic comparators use photoelectric settings. The large machine shown in figure 4-48 may be used in either a manual or automatic mode.

4.8.2 HISTORY

Cameras were first calibrated in the 1930's using visual techniques. Theodolites made acceptably accurate measurements of narrow angle lenses while goniometers were used for wide-angle lenses. When the center of the entrance pupil of the test lens or cone is approximately coincident with the rotation axis of the goniometer, accurate visual measurements may be obtained with monochromatic illumination. The sun, however, is the source of illumination for aerial surveying, making calibration with "white" light more meaningful, if not essential. It is extremely difficult to design and manufacture wide angle mapping lenses covering a 4,000 to 7,000 Angstrom range without some residual

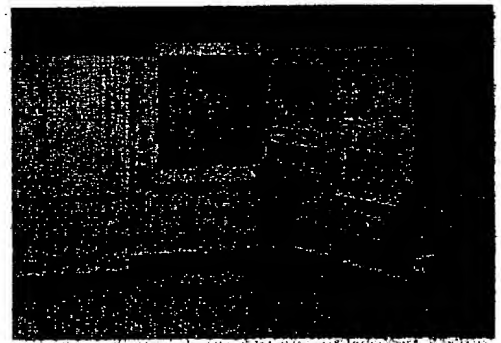

FIGURE 4-48. Mann Type 2405 Automatic Precision Comparator. This high precision comparator is used chiefly for measurement of the X and Y coordinate positions of symmetrical images, as for instance, stars. Selection of image position is manual or photoelectric using closed loop feedback servos. The environment is self-contained, regulating temperature, dust and humidity within normal levels for accurate measurement.

One of the most recent procedures for calibration of the "system," termed the Method of Mixed Ranges (MMR) was invented by Merchant (1974). The method utilizes a three-dimensional control range (mountains), and a conventional flat range, in an adjustment in which the elements of interior orientation are carried as common parameters for all exposures. The use of the three-dimensional range for suppressing high correlations between certain elements of interior and exterior orientation is thought to be unique for the normal aerial case. The author notes that the advantages of the MMR procedure is that no modification to the total "system" is required, other than the choice of the conditional function which includes the parameters of interior orientation.

Merchant's concern is with the calibration of the total "system." With the introduction of reseau cameras, he notes a significant improvement has resulted in film-dimension corrections and the calibration procedures may now be expanded into closer conformance to the concept of "system" calibration.

Anculete and Disconescu (1976), Romania, report a nearly similar method, calling the calibration a "methodology used under normal work conditions." The control points on flat and high ground are again used. Good results in testing and calibration are claimed.

4.8.5.4.3 U.S.G.S. Model-Flatness Test

Before the U.S. Geological Survey awards a contract for aerial photography to a successful bidder, the camera to be used must pass a model-flatness test to insure that stereomodel distortion does not exceed 1/5000 the flight height. In the testing, the U.S.G.S. camera calibrator is used to take photographs on film, simulating aerial photographs. Fifteen of the collimators are set so that a stereomodel can be formed by using one photograph as the left plate of a stereopair and the second photograph as the right conjugate plate (figure 4-57). The stereo model so formed contains nine points (images of collimator targets) that would all lie in a plane if errors were not present (figure 4-58). Because errors are present, the nine points appear to lie in different planes. From measured plate coordinates of the images, U.S. Geological Survey first calculates the translations and rotations necessary to make the coordinate system of the right-hand photograph parallel to that of the left-hand coordinate system with its origin the length of the air base from the origin of the left-hand photograph's coordinate system. A plane is then fitted by least-squares to the nine points in the stereoscopic model, and the difference between the measured z-coordinate and the corresponding z-coordinate on the plane calculated. If any of the nine differences exceed 1/5000 of the focal length of the camera, that camera is rejected.

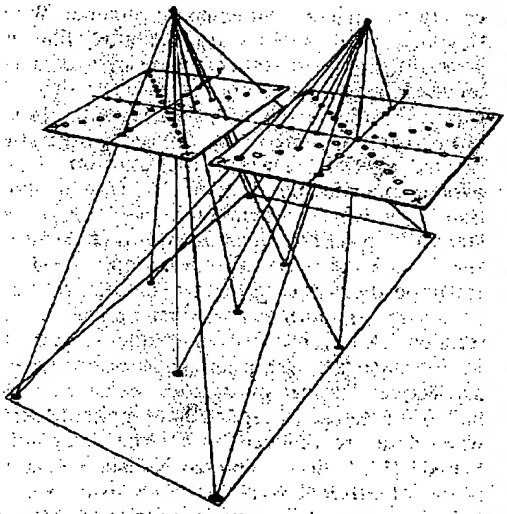

Figure 4-57. A stereopair of camera-calibrator plates containing nine conjugate points.

4.8.5.5 Calibration of Close-Range Cameras

In contrast to aerial cameras, for which laboratory and field calibration procedures have remained the same over the years and for which standard procedures have been recommended, no standard calibration procedures exist for close-range cameras. Another major difference between these types of cameras is that both metric and nonmetric cameras are used in close-

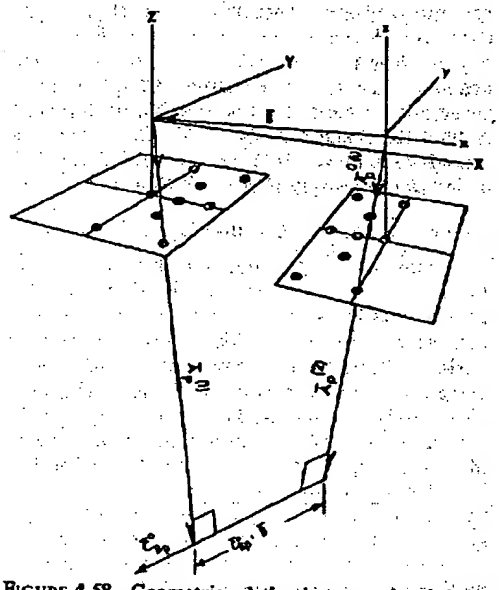

Figure 4-58. Geometric relation between the air base of a stereopair, two rays through corresponding images, and a vector perpendicular to the two rays.

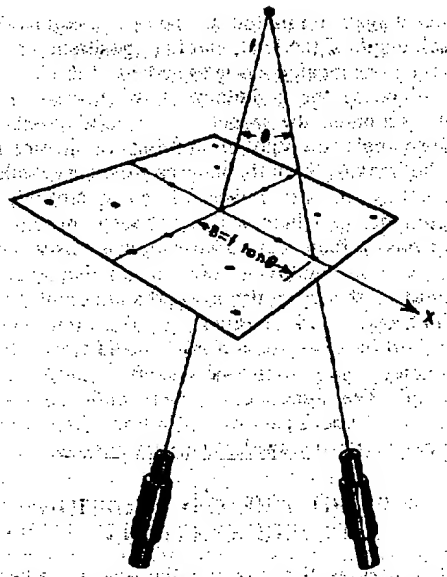

FIGURE 4-59. In order to form a stereomodel at photograph scale, the magnitude of the air base B is computed as the distance at photograph scale from the center target of the left photograph to the outermost target along the flight line. This outermost target corresponds to the center target on the conjugate photograph.

range photogrammetry. In most cases, the optical laboratory methods involving the use of goniometers, collimators, multicollimators, *etc*, are not suitable for close-range camera calibration since such cameras are usually focused (or focusable) at finite distances. As a result, a number of ingenious approaches for calibration of close-range cameras have emerged. Depending on the accuracy requirements in photogrammetric measurements, various degrees of sophistication can be used to define the interior orientation of close-range cameras, ranging from the simple classical approach involving only the reconstruction of the position of the interior perspective center to the highly refined analytical solutions wherein the radial and decentering lens distortions, film deformations, affinity as well as the variation of the lens distortion with

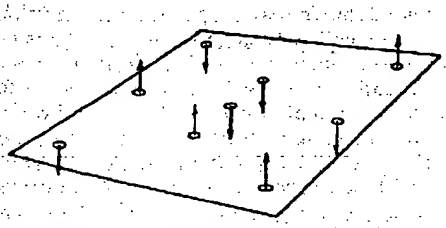

FIGURE 4-60. A regression plane fitted to nine points in a stereomodel. The circles represent the intersection of the error vectors and the regression plane.

object distance within the photographic field are taken into consideration.

Calibration is usually carried out in one of three fashions: in the laboratory, on the job, and by self-calibration. Metric cameras are ideally suited for laboratory calibration. Three-dimensional test objects of various kinds have been used, *e.g.*, Abdel-Aziz & Karara (1974), Döhler (1971), Faig (1971), Malhotra & Karara (1975), Torlegård (1967), Wolf & Loomer (1975). The mathematical formulation is generally based on the collinearity equations. Five object-space control points are required to solve for the principal point and principal distance. With the inclusion of additional unknowns, the number of object-space control points has to be increased, *e.g.*, Abdel-Aziz & Karara (1974), Faig (1971), Karara & Faig (1972), Torlegård (1967). The basic resection approach fails for telephoto lenses with cone angles of 2° or less. Merritt (1975) has overcome this problem by applying the Hartman method.

On-the-job calibration utilizes photography taken of the object and of the object-space control simultaneously. At least one full (X,Y,Z) object-space control point should be provided for every two unknown quantities included in the solution. The mathematical formulation is essentially the same as used in laboratory calibration. Several approaches have been reported in the literature on the construction of special control frames which maintain their geometric configuration sufficiently well to be used for control purposes, *e.g.*, Böttinger (1972), Brandow *et al* (1975), Faig (1974), and others.

Although not explicitly a calibration method, the *D*irect *L*inear *T*ransformation (DLT) method developed at the University of Illinois (*see e.g.* Abdel-Aziz & Karara 1971, 1974) is generally regarded as an on-the-job calibration method. In this method, the solution is principally for the interior orientation of the individual images but the elements themselves are not explicitly obtained from the solution of the equations. The DLT method is particularly suitable for non-metric photography which has no fiducials, since the solution is based on the concept of direct transformation from comparator coordinates into object-space coordinates, thus bypassing the traditional intermediate step of transforming from a comparator system to a photo-coordinate system. The minimum number of unknowns in the solution is eleven (11), but these can be increased to take into account additional unknowns. The recommended mathematical model (Karara & Abdel-Aziz (1974)) involves 12 unknowns, thus requiring a minimum of 6 object-space control point images in the photograph.

The self-calibration approach does not require object-space control as such for the calibration. Multiple (at least 3) convergent photographs are taken of the object. Using the complanarity con-

dition equations and well-defined object points, elements of interior orientation are computed for the camera used, assuming that the elements remain unchanged between photographs. This method is well documented in the literature, *e.g.* Brown (1971, 1972), Kolbl (1972). A self-calibration method which permits the determination of the elements of interior orientation for each photograph has been developed at the University of New Brunswick (Faig, 1976). This method is applicable to metric as well as to non-metric photography.

4.8.5.6 Calibration of Underwater Cameras

Calibration of underwater cameras is done using a multicollimator instrument designed by McNeil (1972), and similar in principle to that originally developed by Washer and Case of the National Bureau of Standards (1949). The distance at which an underwater camera can photograph an object is limited by the turbidity of the water. The focus of each collimator must therefore be easily adjustable to simulate an object distance from six feet to infinity. Like a theodolite, the adjustment must be accomplished without a change in pointing angle. The reticles of the collimators have both fiducial crosses marking the angle and resolution reticles. As the object distances are adjusted in the collimators, the resolution values will change as a function of ratio of collimator to camera focal length.

Both the calibrator and the cameras, with well sealed windows, are under water, preferably water of the same type and clarity as that in which the cameras will be used (*e.g.*, sea water of various clarity). Detailed mathematics and calibration techniques are available in a small book, "Optical Fundamentals of Underwater Photography," McNeil (1972).

Merritt (1974) developed a theoretical basis for calibration of underwater cameras by applying methods for calibration of aerial cameras. The key to the observational procedure is to establish coplanarity between the water surface and the camera focal plane. The refraction angles are then corrected for the air-water interface. Only the camera lens is immersed in a shallow pool of water. Collimators in air, below the pool, are pointed so that their rays, refracted first by the glass window of the pool and then by the water, are incident on the lens in the camera. An auto-collimator, again in air, is mounted vertically above the camera. A simple pool with a plane-parallel plate bottom could easily fit on an infinity-focused calibrator if a 35 or 50 mm underwater camera were to be used.

4.8.5.7 Calibration of Panoramic Cameras

Panoramic cameras have "built-in" distortions due to the camera design. If the design is such that during exposure the film is held stationary against a platen whose radius equals the focal length of the lens, carefully positioned fiducials can be located along the edges of the format to reference the geometry of the format. The lens, scanning the targets of a multicollimator whose angles are known, provides the geometry of the images. Such techniques can be expanded to include the correction for image motion. A second design which requires that the motion of film past a fixed slit move synchronously with the scanning rotation of a prism can also be calibrated. In this case, timing marks are employed. Film transport which might vary from ten to one hundred inches a second might need timing frequencies higher than one thousand cycles per second. The dynamics of panoramic cameras suggests the necessity of calibration with several frames being analyzed at various speeds.

4.8.7 FUTURE CALIBRATION CONSIDERATIONS

The various methods of calibration have been discussed in previous paragraphs, each method having specific advantages. The multicollimator method has high production capability and every phase can be well controlled. The laboratory goniometer techniques are also precise and well controlled when corrections are made for visual chromatic aberrations. Stellar methods have high accuracy by virtue of the dense field of stars of known positions. Camera "system" tests which include the uncontrolled (or partially controlled) environment of the airborne vehicle may appear most realistic but the use of the calibration values so derived needs proof in a reasonable number of applications.

The question as to which method best serves the interest of the map-makers is not yet answered. It begins to be apparent, however, that two additional studies are still needed to evaluate the complete problem. One study should correlate geometry from images on glass plates with geometry from images on film in the operational camera. To explain: there has been general acceptance that the operating camera system is a highly stable instrument geometrically, and unless one is concerned with geometric accuracy to a few micrometres, this assumption is tenable. When, however, isolated tests have shown that good agreement in values of separate calibrations on plates and film is not always attained, then it would seem that the next step in calibration should be a requirement for this test. The operating camera calibration should not be a substitution for calibration of the camera body since this is basic, the role of the national laboratories in quality control of mapping cameras is fundamental, but it should be an additional calibration that requires agreement of geometric values. The stability of the operating camera geometry is then more nearly assured. Such was the path that lead Hallert to his Tall